Water Research 141 (2018) 329–339

Contents lists available at ScienceDirect

Water Research

journal homepage: www.elsevier.com/locate/watres

Reducing phosphorus (P) losses from drained agricultural fields with iron coated sand (- glauconite) filters

Stany Vandermoere [a, *], Njaka Andriamanantena Ralaizafisoloarivony [a], Eric Van Ranst [b], Stefaan De Neve [a]

[a] Department of Soil Management, Faculty of Bio-Science Engineering, Ghent University, Coupure Links 653, 9000 Ghent, Belgium
[b] Department of Geology, Faculty of Sciences, Ghent University, Krijgslaan 281 (S8), 9000 Ghent, Belgium

ARTICLE INFO

Article history:
Received 2 February 2018
Received in revised form
4 May 2018
Accepted 13 May 2018
Available online 16 May 2018

Keywords:
Water quality
Water framework directive
Phosphorus
Eutrophication
Tile drainage
Phosphorus sorbing materials

ABSTRACT

In north-west Europe, agricultural diffuse P losses are a major cause of eutrophication problems in surface waters. Given that the Water Framework Directive (WFD) demands fast water quality improvements and most of the actual P mitigation strategies tend to work on the long run, new short-term mitigation measures are urgently needed. We here report on the entire process of developing small scale field filters to remove P at the end of tile drains, starting from the screening of potential P sorbing materials (PSM): iron coated sand (ICS), acid pre-treated natural minerals (biotite, glauconite and olivine) and bauxite. Initial batch (ad)sorption experiments revealed following order in both, P sorption capacity and speed: ICS > bauxite > glauconite > olivine = biotite. Because of the presence of significant amounts of lead and/or nickel, we excluded bauxite and olivine from further experiments. Subsequent lab scale flow through systems were conducted with P filters containing mixtures of ICS and glauconite (100/0, 90/10, 80/20, 70/30 and 60/40%, respectively, on weight basis). We found a significant relationship between K_{sat} and the filter mixtures particle size distribution and bulk density, and a significant effect of the filter mixture composition on P removal efficiency and stability of K_{sat}. During the 10 week field trials, the pure ICS filters were capable of processing all drainage discharge rates (up to 6 m^3 day^{-1}) with a P removal efficiency of ≥74%. The 90/10 ICS/glauconite filters could process up to 4 m^3 water day^{-1} with a P removal efficiency of 57%. As saturated ICS filters can easily be replaced and recycled for other applications, this is a promising sustainable technique to drastically cut back diffuse P losses and to tremendously improve surface water quality in the short term.

1. Introduction

Since the late 60s and 70s agriculture in north-west Europe has intensified strongly. The concomitant increase in livestock units and use of (mineral) fertilizer has led to highly positive nutrient balances at field level (Correll, 1998; Ulen et al., 2007), resulting in the accumulation of nutrients such as phosphorus (P) in soils and high P saturation degrees. This is especially the case in Flanders (Belgium), The Netherlands (Chardon and Faassen, 1999; Schoumans and Chardon, 2015) Denmark, and parts of e.g. France (Brittany), Spain (Catalunya) and Italy (river Po plain). An even stronger and much more rapid intensification has been observed also in some regions of China (e.g. Changsha) (Qin et al., 2010). In Flanders and The Netherlands losses of P via erosion, run-off and leaching account for almost 60% of the eutrophication problems (Groenenberg et al., 2013).

In order to meet the requirements of the Water Framework Directive, these P losses need to be mitigated urgently. Whereas P losses by erosion and run-off can be cut back very efficiently by means of catch crops, buffer strips and reduced tillage (Chambers et al., 2000; Salomez et al., 2006), there are no efficient

Abbreviations: P, Phosphorus; WFD, Water Framework Directive; PSM, Phosphorus sorbing material; SSA, Specific surface area; K_{sat}, Saturated hydraulic conductivity; ICS, Iron coated sand; ICP-OES, Inductively coupled plasma optical emission spectrometry; D_x, Grain size diameter where x % of all particles are finer by weight; BD, Bulk density; V, Discharge volume; L, Length of the filter column; A, Cross sectional area; t, Time; Δh, Water head difference; Q_e, Sorbed phosphorus at equilibrium; C_e, Phosphorus concentration at equilibrium; Q_{max}, Maximal P sorption capacity; K_a, Phosphorus affinity parameter; S_P, Sorbed phosphorus; S_{Pmax}, Maximal kinetic P sorption; K, Phosphorus sorption rate parameter.

* Corresponding author.
E-mail address: stany.vandermoere@ugent.be (S. Vandermoere).

https://doi.org/10.1016/j.watres.2018.05.022
0043-1354/

management practices to reduce P leaching on the short term. Reduction of P leaching losses is generally believed only to be possible on the long run (decadal time scale) by means of phytomining and reduced fertilizer use (van der Salm et al., 2009; Nest et al., 2015).

However, there may be one specific case of P leaching with a large mitigation potential. In tile drained agricultural fields, the drains short-circuit the P buffering capacity of the subsoil, resulting in high loads of P (sometimes up to 5.0 ppm P) that are discharged directly into the surrounding surface waters (Sims et al., 1998; McDowell and Sharpley, 2001). For this type of P losses, four potential mitigation options exist (Buda et al., 2012). A first option is the installation of P filters in the receiving waterbodies (Bryant et al., 2012), but due to the high clogging risk of these filters, this option seems to have very a limited practical applicability. A second option consists of backfilling the trenches of newly installed drainage tubes with P sorbing materials (PSM) (McDowell et al., 2008; Groenenberg et al., 2013). Although this option can reduce P losses to almost zero, it can only be used for newly installed drains, and requires very large amounts of PSM (typically 100–200 tonnes ha^{-1}), which cannot be recovered from soil. Moreover, P leaching may recommence once the PSM is saturated. A third option is installing small constructed wetlands filled with a PSM at the end of the drains. These systems can remove both particulate and dissolved reactive P, but require a size up to 8% of the catchment area and have a highly variable P removal efficiency (1–88%) (Brooks et al., 2000; Braskerud et al., 2005). A fourth mitigation option consists of installing P filters at the end of the drains, in the edge of the field (Penn et al., 2007). This allows circumventing problems of the other mitigation options, but presents a number of technical challenges which to date have prevented its use in practice. The biggest challenge is to develop a filter system that combines large hydraulic conductivity (to accept peak drainage flows) with high P removal efficiency (with minimal reaction time).

Whichever of the four options above is selected, the P removal structure should primarily have a high P sorption affinity (i.e., react fast) and have a long lifespan (i.e. feature a high P sorption capacity). There should also be no appreciable P desorption from the PSM when P concentrations in the drainage water decrease. These properties are basically determined by the combination of elemental composition and specific surface area (SSA) of the PSM. PSM with a high Fe, Al and Ca content and a large SSA show the best P removal (McDowell et al., 2008; Buda et al., 2012). In addition, the costs of producing, installing and maintaining a P removal structure should be minimal. Therefore, it should be considered per region or even per site whether the use of secondary materials (e.g. iron coated sand), natural minerals (i.e. abundantly occurring minerals rich in iron, aluminium or calcium) or engineered materials is the most suitable option (Penn et al., 2007; Egemose et al., 2012). Finally, the P removal structure should be capable of processing peak flows, which contain the highest P loads. As the available space for P removal structures is often limited, PSM with a relatively high saturated hydraulic conductivity (K_{sat}) should be selected. In order to maintain this high K_{sat} the PSM needs to be physically stable (Moelants et al., 2011; Egemose et al., 2012).

Because of the potentially wide applicability of P filters installed at the end of tile drains compared to other P removal options, we focus on this specific mitigation option. To date research dealing with the development and use of this type of filters has shown a very high P removal potential of typically >80% at lab scale, but a low to moderate P revomal potential of 9.5–60% at field scale (Ayoub et al., 2001; Hylander et al., 2006; Penn et al., 2017). . Because in north-western Europe an important share of the arable land is drained, e.g., 34.5% in the Netherlands, 30% in the UK, 40% in the Scandinavian countries and 17% in Flanders (Belgium) (Van Hecke, 2003; Svanback et al., 2014), and thus at risk of high P leaching, there is a tremendous potential of tile drain filters for water quality improvement.

In this study we wanted to develop and test P filters under laboratory conditions, and validate the filter performance under field conditions. To this end we (i) characterized and tested potential PSM for their P sorption capacity and efficiency in batch experiments, (ii) tested two filter compositions in combination with the best PSM for their P removal performances under a continuous flow experiment and (iii) did a field scale evaluation of the final filter designs.

2. Materials & methods

2.1. Filter materials

We screened ICS, a secondary waste product, three widely occurring natural minerals (biotite, glauconite and olivine) and bauxite, an aluminium ore which consists of several minerals, as potential PSM.

The ICS used is a by-product of the drinking water production centre of Pidpa (situated in Grobbendonk, Belgium). When groundwater, which is generally anaerobic, is pumped-up from a deep aquifer, reduced iron (Fe^{2+}) is oxidized. This iron needs to be removed because it can result in clogging of the distribution pipelines and affects water quality negatively (odour, colour and staining). Therefore the water is lead over a sand filter, whereby $Fe(OH)_3$ precipitates on the sand kernels, giving origin to the ICS.

Bauxite, biotite, glauconite and olivine are abundantly available (mixtures of) minerals and can be easily mined in large quantities. Their main constituents are iron, alumina, magnesium and silica, which make them potentially suitable as PSM. However, in bauxite, biotite, glauconite and olivine these ions are a structural part of the crystal lattice, largely unavailable for surface reactions, which only become available over the long term through weathering processes. In order to make these ions available for P sorption reactions, we subjected them to a pre-treatment that simulated enhanced weathering. The minerals were ball milled, followed by acid pre-treatment with HCl (37, 1:3 ratio) for 2.5 h, washed with distilled water and then oven-dried (De Bolle, 2013). The physical pre-treatment caused an decrease in particle size, leading to a higher SSA of the natural minerals. The chemical weathering increased the number of reactive sites available for P sorption (Lyngsie et al., 2014).

2.2. Lab scale experiments

2.2.1. PSM characterization

2.2.1.1. Elemental and mineral composition. For the determination of the full elemental composition of the PSM, 1 g of the samples was filled in platinum crucibles and combusted in a muffle furnace at 850 °C for 30 min. Then the samples were mixed thoroughly with 2 g of lithium metaborate powder and fused for 15 min at 950 °C. The resulting residue was dissolved in a 4% nitric acid solution. Elemental analysis was then performed by inductively coupled plasma optical emission spectrometry (ICP-OES).

For determination of the mineralogy, powder samples were used as starting material. X-ray diffraction (XRD) patterns of the samples were collected on a Philips X'PERT SYSTEM with a PW 3710 base diffractometer, equipped with a Cu tube anode, a secondary graphite beam monochromator, a proportional xenon filled detector, and a 35 position multiple sample changer. The incident beam was automatically collimated. The irradiated length was 12 mm. The secondary beam side comprised a 0.1 mm receiving slit, a soller slit, and 1° anti-scanner slit. The tube was operated at 40 kV and

30 mA, and the XRD data were collected in a theta, 2-theta geometry from 3.00′ onwards, at a step of 0.020° 2-theta, and a count time of 1 s per step.

2.2.1.2. Phosphate sorption isotherms. For the determination of the phosphate sorption isotherms 1 gram of the PSM (0.1 g for the ICS) was shaken on a rotational shaker with 20 ml of a 0.01 M $CaCl_2$ solution containing seven different initial P concentrations between 5 and 100 ppm P prepared from a KH_2PO_4 stock solution (= 1000 ppm P). The 0.01 M $CaCl_2$ solution was used to mimic the ionic strength of the soil solution (McDowell et al., 2008).

After 24 h of shaking, the test tubes were centrifuged at 1500 g for 15 min and filtered on a 0.45 μm Whatmann glass micro filter. Dissolved P present in the supernatant was measured using the method of Murphy & Riley (Murphy and Riley, 1986). For each sample this procedure was performed in triplicate.

2.2.1.3. Phosphate sorption kinetics. Phosphate sorption kinetics of the PSM were determined in a 0.01 M $CaCl_2$ solution containing a low (0.5 ppm P) and high (5.0 ppm P) P concentration. 1 g of the PSM (0.1 g of the ICS) was shaken for 4, 20, 100 and 500 s in 20 ml of the prepared solutions. Immediately after shaking the samples were filtered on a 0.45 μm Whatmann glass micro filter, applying a vacuum, in order to minimize additional P sorption during filtration.

Dissolved P present in the resulting liquid samples was determined using the method of Murphy & Riley (Murphy and Riley, 1986). Each test was performed in triplicate.

2.2.2. Filter development at lab scale

2.2.2.1. Preparation and characterization of filter mixtures. The most promising PSM (as resulting from the P sorption characteristics) were used to prepare filter mixtures, which were further characterized and tested in filters at lab scale. These mixtures were made in order to optimize the hydraulic conductivity and increase the retention times (and hence P removal) in the filters. The ICS was mixed with ball milled and acid pre-treated glauconite in ratios of 60/40, 70/30, 80/20, 90/10 and 100/0% based on weight basis. A small portion (100 g) of the mixtures was used to determine the particle size distribution as described by Canga et al. (2014). This portion was sieved over a range of sieves with mesh sizes varying from 5.00 to 0.05 mm. By weighing the amount of filter material left on each sieve, D_x (D_{10} to D_{90}) values were derived (with D_x being the mesh size of a sieve that allows x % of the filter mixture to pass).

We then prepared filters at lab scale with these mixtures. To determine the bulk density and K_{sat} of the filter mixtures, the mixtures were filled in plastic tubes (length: 30 cm, inner diameter: 60 mm), closed at the bottom with a sintered glass plate (type Robu, porosity: 00), to a height of 20 cm. The bulk density of the PSM was calculated from the empty and filled tubes. Then the filled tubes were placed underneath a downward oriented volumetric flask, to determine the K_{sat} (Fig. 1). By positioning the outlet of the volumetric flask directly under the ponding water level on the filter material a constant water head was created (Klute, 1965). After the first liter of water had passed the filter, the discharge through the filter was recorded in three consecutive periods of 1 min. The K_{sat} values were then calculated as follows:

$$K_{sat} = \frac{V^*L}{A^*t^*\Delta h} \quad (1)$$

with V: the liquid volume passing through the filter, L: the filling height of the filter tube, A: the cross sectional area of the filter, t: the time period and Δh: the water head (in our situation 0.25 m).

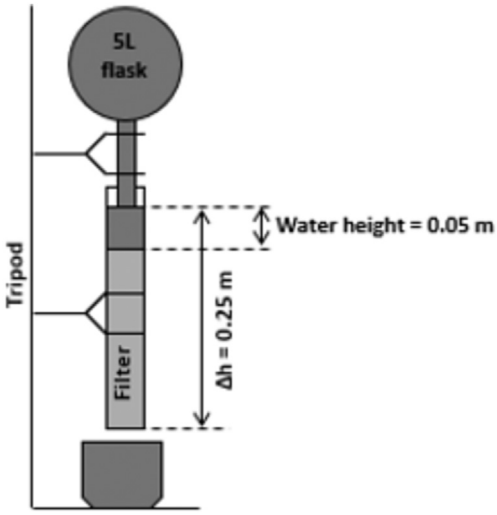

Fig. 1. Setup for determination of saturated hydraulic conductivity of filter materials by means of constant head method (dark grey = water, light grey = filter material).

2.2.2.2. Evolution of K_{sat} and P removal efficiency of filter mixtures. Following discussions on practical filter design and limitations with experimental research stations active in monitoring artificial drainage discharge from agricultural fields, it was concluded that a filter system should not exceed a total volume of 0.072 m^3 (length x width x height = 0.4 m × 0.4 m x 0.45 m) to allow easy installation and maintenance. These preset filter dimensions combined with the expected peak flows (8 m^3 per drainage tube per day (d^{-1})) and the maximum available water head difference (0.25 m), yielded a minimal needed K_{sat} (= 4.5×10^{-4} m s^{-1}) of the PSM. Based on the measured K_{sat}, only the filters containing pure ICS and ICS/glauconite mixtures of 10 and 20% glauconite were used in further experiments (for a more detailed description of filter dimensioning see supplementary materials – S1).

For these filter types a filter system at lab scale was developed as shown in Fig. 2. In this system a 0.01 M $CaCl_2$ solution containing 0.50 ppm P (a concentration considered common in agricultural drainage water in Flanders) was pumped from a large supplier vessel towards a smaller buffer vessel in which the water height was kept constant. The solution was led over the filters at a constant water head via a supplier tube. The water head difference (Δh) for each filter type was adjusted (varying from 0.05 m for the pure ICS filter to 0.25 m for 80/20% ICS/glauconite filter) in such a way that all filters could be tested under the same peak flow conditions.

The evolution of K_{sat} and P removal efficiency were monitored by determining the K_{sat} of the filters and the residual P present in the effluent each time 10 liter had passed the filters.

2.2.2.3. Field scale experiments. Field scale filters, with either pure ICS or the 90/10% ICS/glauconite mixture as PSM, were built using 65 liter PVC vessels (Fig. 3). The 80/20% ICS/glauconite filter was not included during field trials because both the K_{sat} and P removal efficiency of this filter strongly decreased over time, during the lab scale tests. In these vessels a large construction sieve (diameter: 45 mm, mesh size: 40 mm) was placed on a wooden support and glued to the edges. By covering the sieve with a meshed netting (type: AISI316, mesh size: 50 μm) a dense and firm support for the PSM was obtained. A hole was drilled at the bottom of the PVC vessel and connected to a discharge tube. Depending on the PSM (pure ICS or a 90/10% ICS/glauconite mixture) the discharge tube was led upwards (low constant head difference of 0.05 m) or left at the bottom (high constant head difference of 0.25 m). At the top of

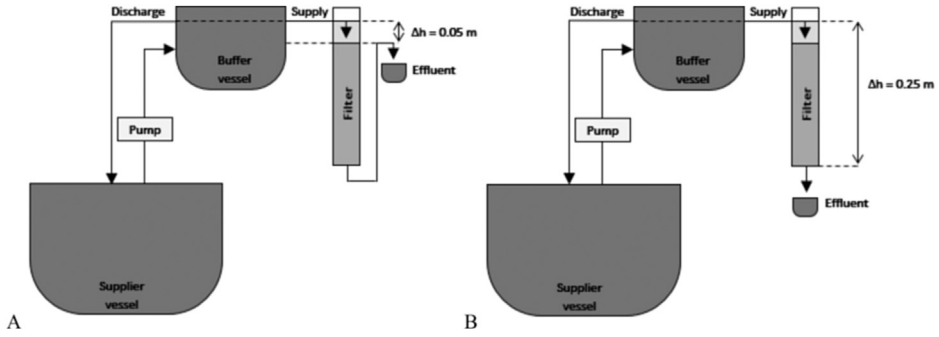

Fig. 2. Filter conformations at lab scale for filters containing (A) only ICS and (B) filters containing 80/20% ICS/glauconite.

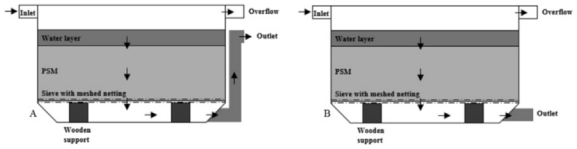

Fig. 3. Schematic overview of field scale filters when using (A) pure ICS, (B) 90/10% ICS/glauconite as PSM.

the vessel another hole was drilled and connected to an overflow. This allowed to keep the drain running in case the filter would clog.

Filters were tested at four sites during 10 weeks in the winter of 2016 and/or 2017. The sites were selected based on two criteria, namely a ortho-P concentration in the drain water higher than 0.10 mg P L^{-1}, and the end of the tile drain had to be above the water level of the ditch. As in many situations the space between the drainage tube and the water level of the ditch was small (≈0.10 m), the filter with 90/10% ICS/glauconite with the downward oriented discharge tube (filter 4) could only be tested at one site. Concentrations in the drainage water varied from 0.10 to 0.40 mg ortho-P L^{-1}.

Monitoring of the filters was done on a weekly basis and consisted of discharge measurements from the filter outflow and sampling of the filter in- and outlet. The filter discharge was determined by recording the time (in triplicate) to collect two liters of water. The water samples were put in a glass jar and stored in a cooling box for transport. Upon arrival in the lab, the dissolved reactive P (DRP) content of the water samples was determined immediately, using the method of Murphy & Riley (Murphy and Riley, 1986). Total P and total dissolved P were not determined, as preliminar screening had shown that most P present (≥90%) in the water samples consisted of DRP (for more information see supplementary material – S2).

2.3. Data analysis

The P sorption isotherms were obtained by plotting the sorbed P (Q_e) versus the solution equilibrium concentration (C_e) and fitting the Langmuir equation (equation (1)) to these data.

$$Q_e = \frac{Q_{max} * K_a * C_e}{1 + K_a * C_e} \quad (2)$$

For the P sorption kinetics experiment the amount of P sorbed was plotted against time and fitted to following hyperbolic equation:

$$S_P = \frac{S_{Pmax} * t}{K_f + t} \quad (3)$$

where S_P is the amount of sorbed P in time (t), S_{Pmax} is the maximum amount of P that can be sorbed and K_f is a curve fitting parameter related to the P sorption rate.

The D_x values and bulk densities of the filters at lab scale were used as independent variables in a stepwise regression analysis with K_{sat} as dependent variable. This should allow to estimate the K_{sat} of future batches of PSM.

All curve fittings and statistical analyses were performed with the R software package (R_Core_Team, 2017).

3. Results

3.1. PSM characteristics

3.1.1. Elemental and mineral composition

The olivine used in this study is a forsterite and contains iron (Fe) (7.9% Fe_2O_3) as main P sorbing element (Table 1). Despite its potential for P sorption, olivine contains very high amounts of nickel (Ni = 3053 mg kg^{-1}) which might pose an environmental risk. ICS is clearly dominated by Fe (62.5% Fe_2O_3) as P sorbing element. The biotite used in this study is a phlogopite containing Fe and aluminium (Al) in almost equal amounts (8.7% Al_2O_3 and 8.7% Fe_2O_3) and a substantial amount of calcium (Ca) (9.4% CaO). Because biotite does not contain any Ca, we assume that traces of $CaCO_3$ were present in the biotite sample we used. In bauxite Fe (41.1% Fe_2O_3) predominates over Al and Ca (23.1% Al_2O_3 and 10.4% CaO). Further large amounts of lead (Pb = 187 mg kg^{-1}) and nickel (Ni = 826 mg kg^{-1}) are present in bauxite, which might pose environmental risks. In glauconite Fe (13.3% Fe_2O_3) and Al (6.1% Al_2O_3) act as the main P sorbing elements, with hardly any Ca or Mg (for a more detailed description of the XRD pattern determination of the PSM and findings on the obtained results see supplementary material – S3).

3.1.2. P sorption isotherms and kinetics

The ICS had by far the largest P sorption capacity (Fig. 4 and Table 2). With a Q_{max} value of 10 510 mg P kg^{-1} filter material it sorbed highly significantly ($P < 0.0001$) more P than the other PSM, which had a Q_{max} in the order (significant at $P < 0.05$): bauxite > glauconite > biotite = olivine.

The K_a values of olivine and biotite (0.132–0.060 liter mg^{-1}, respectively) were highly significantly larger ($p < 0.01$) than for the other PSM (Table 2).

The combined effect of Q_{max} and K_a is shown with the Q_e values calculated at a C_e value of 50 mg P L^{-1}. This clearly shows that ICS has by far the best P sorption properties, followed by pre-treated

Table 1
Mineral and elemental composition of the five potential PSM (bauxite, biotite, glauconite, ICS and olivine).

	Mineral composition (%)										Elemental composition (mg.kg^{-1})						
	SiO_2	Al_2O_3	Fe_2O_3	MnO	MgO	Na_2O	CaO	K_2O	TiO_2	P_2O_5	Cd	Cu	La	Ni	Pb	S	Zn
Bauxite	7.0	23.1	41.1	0.1	0.3	2.8	10.4	0.1	4.2	0.1	<15	52	134	826	187	181	75
Biotite	38.6	8.7	8.7	0.1	19.1	0.6	9.4	7.5	0.3	0.4	<15	9	28	8	<10	180	72
ICS	5.3	0.3	62.5	0.9	0.2	<0.1	6.8	0.1	0.0	4.2	<15	21	25	<0.1	<10	200	<20
Glauconite	68.5	6.1	13.3	0.0	2.0	0.1	0.1	4.8	0.1	0.1	<15-	20	–	13	25	250	50
Olivine	42.0	0.4	7.9	0.1	48.1	<0.1	0.2	0.0	0.0	0.0	<15	7	115	3053	14	212	59

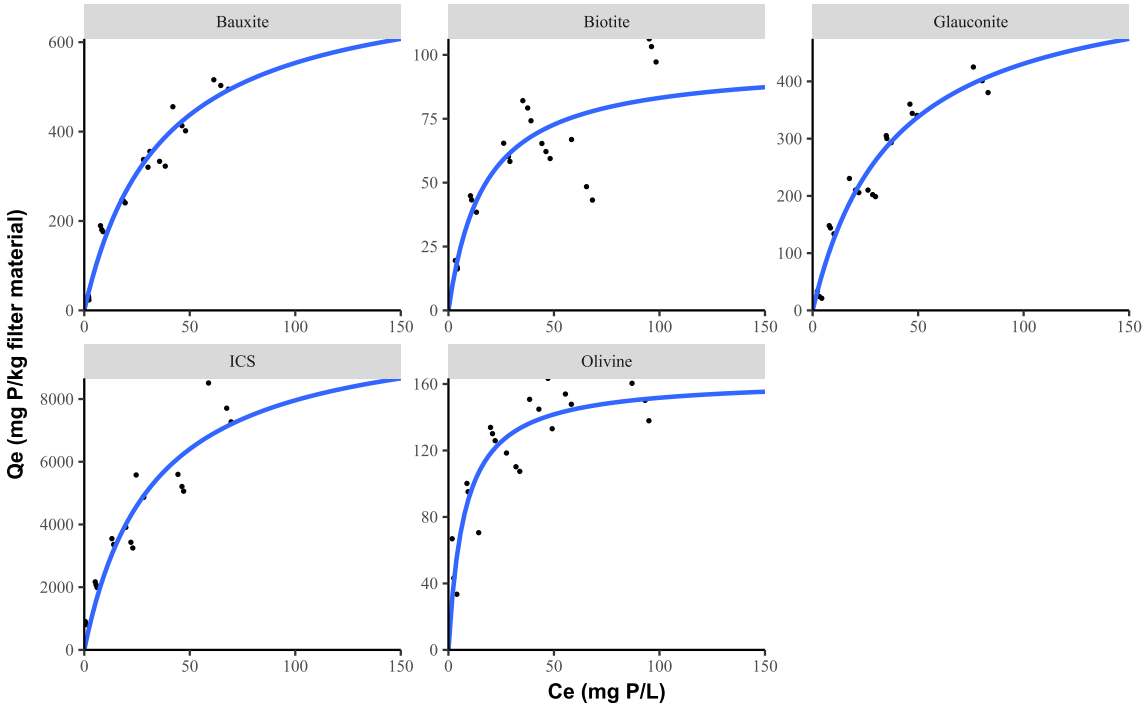

Fig. 4. Q_e and C_e values of the PSM (Bauxite, Biotite, Glauconite, ICS and Olivine) combined with the fitted Langmuir isotherm. Values shown are averages, error bars represent one standard deviation.

Table 2
Parameter estimates of Q_{max} and K_a of the Langmuir equation fitted to the Q_e and C_e values of the PSM (bauxite, biotite, glauconite, ICS and olivine). Standard error of the parameter estimates is shown between brackets. a > b > c > d at the 5 % significance level.

Material	Q_{max} (mg P.kg filter material^{-1})		K_a (L.mg^{-1})		Q_e (mg P.kg filter material^{-1}) (C_e = 50 mg.L^{-1})
Bauxite	754.10^{b}	(69.9)	0.028^{b}	(0.005)	439.89
Biotite	97.10^{d}	(11.9)	0.060^{a}	(0.025)	72.83
Glauconite	594.10^{c}	(58.5)	0.026^{b}	(0.005)	335.80
ICS	10510.00^{a}	(1438)	0.031^{b}	(0.009)	6388.43
Olivine	163.20^{d}	(9.7)	0.132^{a}	(0.036)	141.73

bauxite, glauconite, olivine and biotite.

In the kinetics experiment ICS showed significantly higher ($P < 0.0001$) S_{Pmax} than the other PSM at both low and high P concentrations (Fig. 5 and Table 3), sorbing from 2 to 19 times and 5 to 28 times more P at low and high P concentrations, respectively. Based on significantly different S_{Pmax}, the materials were in the order ICS > bauxite > glauconite > biotite = olivine.

Bauxite and ICS had significantly higher ($P < 0.05$) P sorption rates (K_f values) than the other PSM at low P concentrations. At high P concentrations the differences in P sorption rate were smaller. Based on significantly different K values the materials were in the order bauxite ≥ ICS = olivine ≥ biotite > glauconite (Table 3).

The combined effect of S_{Pmax} and K_f is shown with the S_P value calculated at a t value of 30 s. This shows that ICS has the highest P sorption affinity, followed by bauxite, glauconite, olivine and biotite.

3.2. Lab scale filters

Because of the presence of significant amounts of lead and/or nickel, we did not further include bauxite and olivine in our lab trials. Also biotite was excluded because its P sorption capacity was low. Therefor we decided to focus on ICS for further development of filters on lab and field scale. Furthermore, we decided to also look at combinations of ICS with glauconite as a means of optimizing the combination of minimum needed hydraulic conductivity (to allow peak volumes to be processed) with minimum needed residence time (to allow sufficient reaction time). The

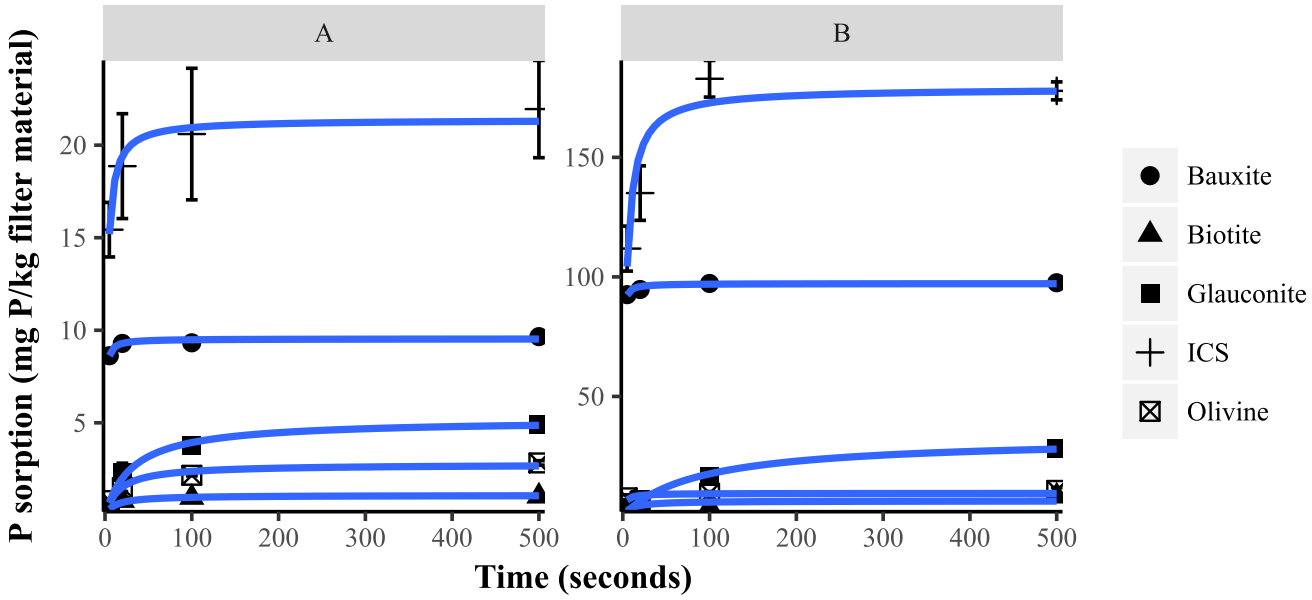

Fig. 5. P sorption kinetics of the PSM (bauxite, biotite, glauconite, ICS and olivine) at (a) low (0.50 ppm P) and (b) high (5.00 ppm P) P concentrations fitted by the hyperbola equation (3). The P sorption values shown are averages, error bars represent one standard deviation.

Table 3
Parameter estimates of S_{Pmax} and K of the fitted hyperbola function (equation (2)) to the P sorption kinetics of the PSM (bauxite, biotite, glauconite, ICS and olivine) at low (0.50 ppm) and high (5.00 ppm) P concentrations. Standard error of the parameter estimates is shown between brackets. a > b > c > d at the 5 % significance level.

P concentration ($mg.L^{-1}$)	Material	S_{Pmax} (mg P.kg filter $material^{-1}$)		K_f (seconds)		S_p (mg P.kg filter $material^{-1}$) (t = 30 s)
0.50	Bauxite	9.50^{b}	(0.10)	0.50^{c}	(0.10)	9.34
	Biotite	1.10^{d}	(0.10)	11.10^{b}	(4.10)	0.80
	Glauconite	5.20^{c}	(0.40)	31.50^{a}	(9.10)	2.54
	ICS	21.40^{a}	(1.70)	2.00^{c}	(1.30)	20.06
	Olivine	$2.80^{c,d}$	(0.10)	16.10^{b}	(3.50)	1.82
5.00	Bauxite	97.20^{b}	(0.30)	0.30^{c}	(0.03)	96.24
	Biotite	6.30^{d}	(0.90)	8.90^{b}	(5.90)	4.86
	Glauconite	32.80^{c}	(1.80)	86.10^{a}	(15.10)	8.48
	ICS	179.00^{a}	(7.40)	$3.60^{b,c}$	(0.90)	159.82
	Olivine	9.50^{d}	(0.90)	$2.10^{b,c}$	(1.60)	8.88

choice for glauconite was based on its local availability and low presence of heavy metals.

3.2.1. Filter characteristics

Decreasing the ratio of ICS over glauconite resulted in a systematic and significant decrease of D_x and K_{sat} values (from 32.33×10^{-4} m s^{-1} for 100/0% to 0.89×10^{-4} m s^{-1} for 60/40%) and a concomitant increase in bulk density (Table 4).

The stepwise regression analysis, with K_{sat} as dependent variable and the D_x values and bulk density as independent variables, led to a final prediction model characterized by three significant parameters: D_{10} ($P = 0.0024$), D_{40} ($P = 0.0433$) and bulk density (BD) ($P = 0.0002$), with K_{sat} expressed in $m.s^{-1}$, D_{10} and D_{40} in mm and bulk density in kg m^{-3}.

$$K_{sat} = 1.50{*}10^{-2} + 1.15{*}10^{-3}\, D_{10} - 8.70{*}10^{-4}\, D_{40} - 1.02{*}10^{-5}\, BD \quad (4)$$

The relation between estimated (with Eq. (3)) and measured K_{sat} (Fig. 6) had a high R^2 value (0.969) and low RMSE (0.0002).

3.2.2. Evolution of K_{sat} and P removal efficiency

Filter characteristics revealed that only filters containing pure ICS and ICS/glauconite mixtures of 10 and 20% glauconite reached a sufficiently high K_{sat} to process peak flows. These filters were then further tested in a continuous system with a larger volume of P

Table 4
Mean values of Dx, bulk density and initial K_{sat} of varying filter mixtures of ICS and glauconite (100/0, 90/10, 80/20, 70/30 and 60/40% ICS/glauconite on weight basis).

Mixture	D_{10} (mm)	D_{20} (mm)	D_{30} (mm)	D_{40} (mm)	D_{50} (mm)	D_{60} (mm)	D_{70} (mm)	D_{80} (mm)	D_{90} (mm)	Bulk Density (x 10^3 $kg.m^{-3}$)	K_{sat} (x 10^{-4} m s^{-1})
60/40	0.14	0.18	0.24	0.47	1.27	1.62	1.97	2.32	2.67	1.44	0.89^{d}
70/30	0.15	0.20	0.39	1.19	1.50	1.82	2.09	2.39	2.71	1.37	$1.97^{c,d}$
80/20	0.18	0.35	1.16	1.42	1.69	1.94	2.19	2.47	2.75	1.29	9.06^{c}
90/10	0.29	1.17	1.43	1.70	1.96	2.18	2.39	2.61	2.82	1.18	18.06^{b}
100/0	1.08	1.31	1.53	1.76	1.96	2.16	2.38	2.60	2.81	1.13	32.33^{a}

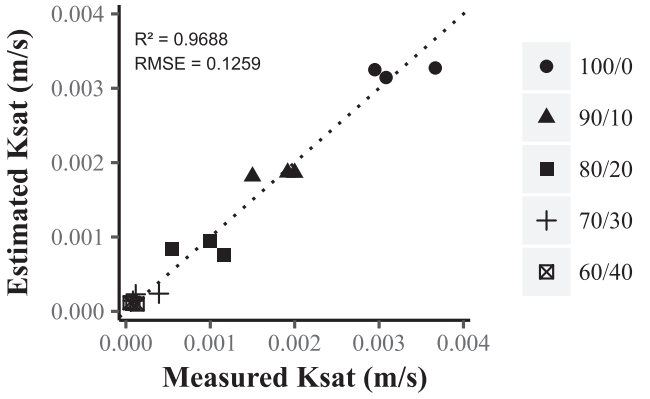

Fig. 6. Comparison of the estimated Ksat (based on the obtained backward stepwise regression equation) and the measured K_{sat} of the filter mixtures of ICS and acid pre-treated glauconite (100/0, 90/10, 80/20, 70/30 and 60/40% ICS/glauconite on weight basis).

containing solution (250 L), equivalent to about 10% of the total amount of solution that passes a drain on average on yearly basis.

As described in section 2.2.2, Δh for each of the mixtures was adjusted in such a way that all tubes processed equal water flows per unit of time (i.e. 1.3 × 10-3 L s^{-1}). This water flow is comparable to peak flow conditions at field level. Under these starting conditions the pure ICS filter had retention times of 220 s, while the 90/10 and 80/20 ICS/glauconite mixtures had retention times of 205 and 186 s respectively. While the 100/0 and 90/10 filters maintained a K_{sat} of at least 2.1×10^{-3} and 1.2×10^{-3} m s^{-1}, respectively, K_{sat} in the 80/20 filter dropped below the level of 4.5×10^{-4} m s^{-1}, which is the minimal anticipated K_{sat} level to process peak flows (Fig. 7). Hence under certain circumstances the 80/20 filters might be unable to process peak flows, which also contain the highest P loads. Furthermore, the K_{sat} of the 80/20 filter varied significantly stronger (coefficient of variation = 32.5%) than the K_{sat} of the 100/0 and 90/10 filters (coefficients of variation of 14.7 and 13.7%), indicating that the 80/20 filter is less stable.

The pure ICS filter performed best in terms of P removal efficiency, with a more or less constant P concentration of 0.03 mg P L^{-1} in the leachate. In the 90/10 and 80/20 filters the P concentration in the leachate tended to increase after 170 and 90 liters respectively. Over the entire experiment the pure ICS filter removed 93.5% of the P passing the filter cumulatively, which was 9.3% (significantly, $P = 0.0070$) higher than the 80/20 filter, whereas there was no significant difference in cumulative P removal with the 90/10 filter.

3.3. Field trials

As the 80/20 ICS/glauconite filter was less stable and removed less P during lab trials, it was decided to conduct field trials with only the pure ICS filter and the 90/10 ICS/glauconite filter. Based on available test sites four filters were built. Each of these filters (filters 1, 2 and 3 = pure ICS filters and filter 4 = 90/10 filter) were tested during a period of 10 weeks, from the second half of November

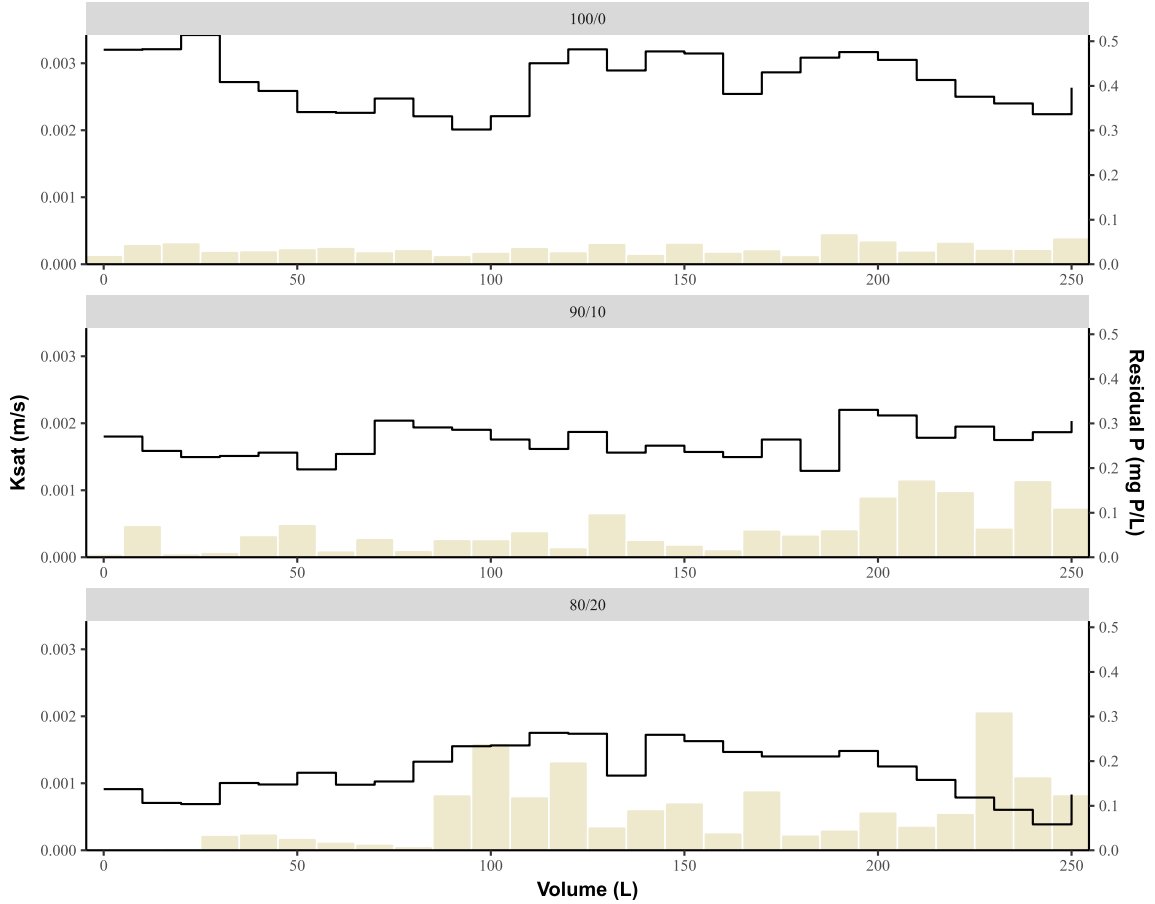

Fig. 7. Evolution of K_{sat} and residual P in the leachate of the tested filters at lab scale (100/0, 90/10, 80/20% ICS/glauconite on weight basis) in function of the volume that passed the filter. The black line represents the evolution of K_{sat}, grey bars show the measured residual P.

until the end of January. During this period the highest precipitation surpluses and drainage discharges were expected.

The pure ICS filters were perfectly capable of processing highly variable drainage discharges (Fig. 8) varying from 0.5 to 1 m^3 of water d^{-1} in dry periods, up to 6 m^3 d^{-1} in very wet periods. This led to retention times varying from 2700 to 226 s. Moreover the pure ICS filters were never flooded by too high drainage discharges. The 90/10 filter was flooded on several occasions (when drainage discharge was >4 m^3 d^{-1}) and processed drainage discharges varying from 2 to 3 m^3 d^{-1}, resulting in retention times of 635 to 424 s.

The pure ICS filters removed 74.1 (filter 1) to 92.4% (filter 3) of the incoming P. These variations in P removal efficiency depended on the drainage discharge rate. In periods of high drainage discharges the residence time of the drainage water in the filter is strongly reduced, leading to a reduction in P removal efficiency, as can be seen for filter 1. Relatively constant drainage discharges, as is the case for filter 2, resulted in constant P removal efficiency. For filter 3 the drainage discharges increased only for a very short period and therefore did not affect the P removal efficiency.

The 90/10 filter removed on average 57.8% of the incoming P. The relatively lower incoming P concentrations and the lower P binding capacity of this filter mixture probably led to a lower P removal efficiency. Bypass flow, occurring when the 90/10 filter was flooded obviously must have further decreased the P removal efficiency of this particular filter, but could not be taken into account.

4. Discussion

A wide range of materials rich in Fe/Al/Ca has been demonstrated to remove P from drainage water both efficiently and at high rates at lab scale (Cucarella and Renman, 2009; Wendling et al., 2013). However, to date field scale applications of P filters containing these materials have proven to be laborious and inefficient in their P removal (Bryant et al., 2012). With the development of small scale field filters, applicable for individual drainage tubes, we

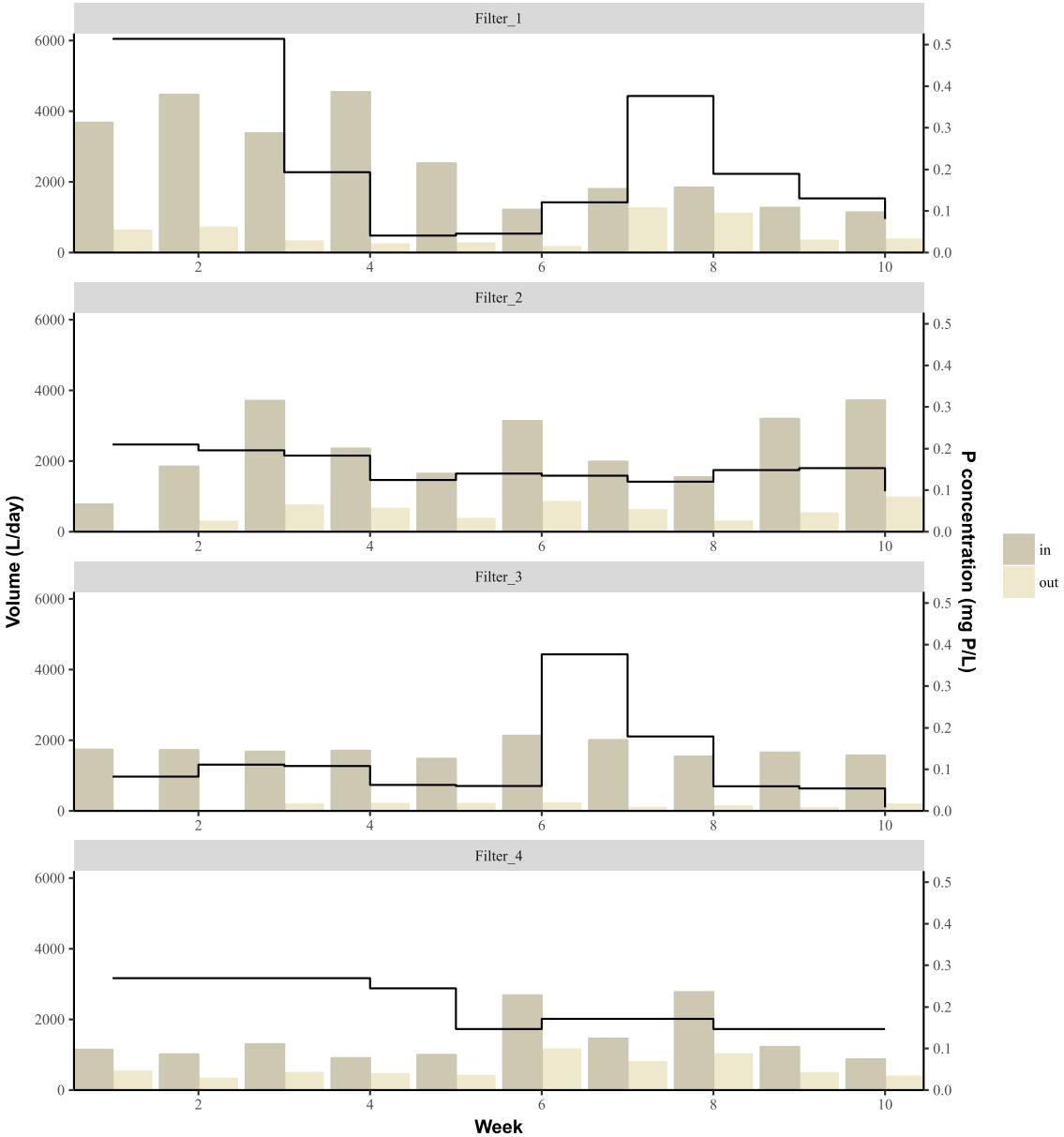

Fig. 8. Performance of P filters at field level. Filters 1, 2 and 3 are filters containing pure ICS, filter 4 contains 90/10% ICS/glauconite. The black line represents the volume processed by the filter, dark grey bars show the incoming P concentrations of the drainage water, light grey bars show the outgoing P concentrations of the drainage water.

demonstrated that P losses via drainage tubes could be reduced greatly and comparable P removal rates and efficiencies could be reached as during lab scale tests.

In our study, screening of potential PSM showed that ICS and natural minerals with Fe as main P fixing element (bauxite and glauconite) outperformed the other PSM in P sorption capacity and rate. Similar P sorption properties for the tested PSM were reported by Moelants et al. (2011), Drizo et al. (1999), Wendling et al. (2013) and Lyngsie et al. (2014). Small differences between these studies and our results are due to variations in the experimental conditions, such as the initial P concentration of the solution and the PSM to solution ratio (Cucarella and Renman, 2009). The Fe rich PSM performed better than the other non Fe dominated PSM because Fe has a stronger hydrolysing power to form chemical bonds with P and it has a higher affinity for P at a slightly acidic pH (Hsu, 1976; Weng et al., 2012). Drainage water originating from acidic sandy soils, which are dominant in our study area, is logically often slightly acidic. Within the Fe dominated PSM, ICS had the best P sorption properties for two reasons. First of all the relative amount of P sorbing elements (Fe/Al/Ca) in the ICS was much higher than in the natural minerals used. Secondly, a much smaller part of the P sorbing elements in these minerals can be made available for surface reactions.

Bauxite and olivine both contain relatively high amounts of Ni and/or Pb. While no short term leaching of Ni and/or Pb from both untreated bauxite and olivine has been reported in literature, the combination of physical and chemical pre-treatment obviously will result in an increased risk of Ni and/or Pb leaching. Moreover, long term leaching risks should then be assessed given the intended time for use of such filter materials in field conditions. We therefore excluded these materials from further testing.

After screening ICS and acid pre-treated glauconite were mixed in diverse ratios to prepare filters at lab scale to monitor the evolution of K_{sat}. The K_{sat} values obtained in our study were in line with the results of Canga et al. (2014), while they strongly exceeded the values reported by Chardon et al. (2012). This observation is explained by the particle size distribution (D_x values), which in our study was comparable to that of Canga et al. (2014) and much larger than that in the study of Chardon et al. (2012), which according to Eq. (3) results in a larger K_{sat}.

Both Eq. (3) and the Canga et al. (2014) equation clearly indicate the small (D_{10}) and medium (D_{40}) particle sizes to be the most important estimators of K_{sat}. In Eq. (3) the small particle size (D_{10}) is positively related to K_{sat} and the medium particle size (D_{40}) is negatively related to K_{sat}. In the equation of Canga et al. (2014) both the small and medium particle sizes were positively related to K_{sat}. The positive relationships are explained by the fact that bigger particle sizes lead to wider pores within the PSM, allowing higher flow rates. The negative relation of K_{sat} with D_{40} in our study may be explained by the fact that relatively coarse particles of ICS (determining D_{40}) were mixed with relatively small particles of acid pre-treated glauconite. These high D_{40} values allow within filter movement of the smaller particles (glauconite) resulting in a heterogeneous pore size distribution of the PSM mixture, which causes a decrease in K_{sat} (Chardon et al., 2012). Furthermore, in our study mixing ICS with glauconite automatically led to an increase in bulk density which seemed to provide additional significant predictive power for K_{sat}. This was not the case in the study of Canga et al. (2014), probably because of the wide range of materials tested. However, Eq. (3) had little predictive power for the K_{sat} values in the study of Canga et al. (2014) ($R^2 = 0.23$), whereas the equation of Canga et al. (2014) quite successfully predicted our K_{sat} values ($R^2 = 0.82$). The equation developed by Canga et al. (2014) thus seems to be more generally applicable.

The K_{sat} of the three filters, with sufficiently high initial K_{sat}, decreased over time during the lab scale continuous flow experiment, but to a variable extent. This decrease was small for the pure ICS and the 90/10 ICS/glauconite filters and was probably caused by aging of the PSM (Sanford et al., 1995). For the 80/20 ICS/glauconite filter the decrease in K_{sat} was more pronounced. We assume that, next to aging of the PSM, this was due to within filter movement of the smaller glauconite particles (Chardon et al., 2012). The P removal efficiency of each filter at lab scale was 80–90%, which is comparable with efficiencies reported by Ayoub et al. (2001). Nevertheless the longevity, i.e. the period that the P concentration in the effluent is below 0.1 mg P L^{-1}, of filters with a larger share of glauconite was lower because of the smaller P sorption capacity (less Fe present) of these filters and shorter retention times in these filters (Burst, 1958).

Small scale field filters were developed to process peak volumes of 6–7 m^3 day^{-1}, based on the K_{sat} values measured at lab scale. However, the 90/10 ICS/glauconite filter could not process volumes larger than 4 m^3 day^{-1}. Next to aging of the PSM, Le Coustumer et al. (2012) found that the influx of sediment and development of algae also reduced K_{sat} of filter systems. A rough estimate in that study showed that a 1/3 reduction of the available pore space reduced K_{sat} with a factor 10. Influx of sediment and growth of algae must also have occurred in the pure ICS filters, and thus must have also reduced K_{sat}, but not to an extent that would limit the water processing capacity, even at peak flows. It could thus be advisable to quantify this potential clogging effect at lab scale. If for practical reasons this is not feasible, then one should take into account a sufficiently large margin in K_{sat} to account for a potential decrease in K_{sat}.

In contrast to the results of Penn et al. (2007) and Bryant et al. (2012), our field scale pure ICS field filters removed from 70 to 90% of the incoming P. Main issues that caused the low P removal efficiencies in these former studies were the occurrence of bypass flow and clogging of the filter system. As the pure ICS filters had a sufficiently large K_{sat} all the incoming water could be processed without any additional maintenance. In addition, our filters had P removal efficiencies comparable to those in the lab scale tests, which is in contrast with results of Ayoub et al. (2001), who noticed a clear decrease in P removal efficiency due to presence of competing species such as sulphates and dissolved organic matter (DOM). In our study sulphates and DOM must have been equally present in the drainage water, and we therefore suspect that the upward orientation of the discharge tube must be the main reason for the superior performance in the field. This upward orientation of the discharge tube indeed ensures an increased filter residence time during periods below peak flow discharges, which allows for an increased reaction time and P removal in the filter.

The lifespan of our small scale field filters depends on two factors: (i) the period during which the filter reduces P losses below the 0.1 mg P L^{-1} limit set by the WFD and (ii) the period during which the filter can process all drainage discharges. Although the lifespan of the pure ICS filters was beyond the period tested in this research, these filters are expected to last shorter than the backfill systems described by Groenenberg et al. (2013) and McDowell et al. (2008). This shorter lifespan is due to the use of much less PSM and the higher flow rates in our filter systems. Nevertheless the PSM in our filter systems can be easily recovered and possibly further used for treatment of other wastewater streams with higher P concentrations and longer filter residence times. Examples include greenhouse wastewater containing P loads varying from 5 to 50 mg P L^{-1} and allowing filter residence times of $\geq$1 h (Westholm, 2006).

Both Ulen et al. (2007) and Grant et al. (1996) state that the amount of DRP in drainage water varies widely (20–85% of total P). Because our field scale filters were only tested in situations where

the amount of DRP was at least 90% of total P, it remains to be seen how efficient these filters would be in situations with higher proportions of particulate P. Up to now, capturing particulate P has only shown to be efficient by constructed wetlands. Nevertheless installing such wetlands is expensive and undesirable in regions where agricultural land is costly (Groenenberg et al., 2013). Therefore the development of a compact filter for particulate P removal may be the next step that needs to be taken to further reduce agricultural P losses in the short term.

5. Conclusions

To date, no efficient mitigation options exist for reducing P concentrations in surface waters, other than reducing erosive P losses. We successfully installed and tested filters for removal of DRP from drain water in field conditions, with a P removal efficiency between 70 and 90%. Such system could be easily optimized for fast and reversible installation at individual tile drains. Given the large area of tile drained fields in areas of intensive agriculture in NW Europe, and the absence of other efficient mitigation options in level areas, this would allow for a rapid and drastic improvement of water quality with respect to P. this would buy time until measures taken at the source (such as P phytomining) start to take effect.

Acknowledgement

This research was carried out within the framework of the NuReDrain project 38-2-17-16, funded by the EU Interreg North Sea programme (38-2-17-16), and the VLAIO LA Trajectory 135080 'A_PROPEAU', funded by the Flemish agency for innovation and entrepreneurship (135080). Further we thank the research stations Inagro, PCG and PSKW which assisted in the design, testing and monitoring of the field scale filters.

Appendix A. Supplementary data

Supplementary data related to this article can be found at https://doi.org/10.1016/j.watres.2018.05.022.

References

Ayoub, G.M., Koopman, B., Pandya, N., 2001. Iron and aluminum hydroxy (oxide) coated filter media for low-concentration phosphorus removal. Water Environ. Res. 73, 478–485. https://doi.org/10.2175/106143001x139533.

Braskerud, B.C., Tonderski, K.S., Wedding, B., Bakke, R., Blankenberg, A.G.B., Ulen, B., Koskiaho, J., 2005. Can constructed wetlands reduce the diffuse phosphorus loads to eutrophic water in cold temperate regions? J. Environ. Qual. 34, 2145–2155. https://doi.org/10.2134/jeq2004.0466.

Brooks, A.S., Rozenwald, M.N., Geohring, L.D., Lion, L.W., Steenhuis, T.S., 2000. Phosphorus removal by wollastonite: a constructed wetland substrate. Ecol. Eng. 15, 121–132. https://doi.org/10.1016/s0925-8574(99)00056-7.

Bryant, R.B., Buda, A.R., Kleinman, P.J.A., Church, C.D., Saporito, L.S., Folmar, G.J., Bose, S., Allen, A.L., 2012. Using flue gas desulfurization gypsum to remove dissolved phosphorus from agricultural drainage waters. J. Environ. Qual. 41, 664–671. https://doi.org/10.2134/jeq2011.0294.

Buda, A.R., Koopmans, G.F., Bryant, R.B., Chardon, W.J., 2012. Emerging technologies for removing nonpoint phosphorus from surface water and groundwater: introduction. J. Environ. Qual. 41, 621–627. https://doi.org/10.2134/jeq2012.0080.

Burst, J.F., 1958. Mineral heterogeneity in glauconite pellets. Am. Mineral. 43, 481–497.

Canga, E., Iversen, B.V., Kjaergaard, C., 2014. A simplified transfer function for estimating saturated hydraulic conductivity of porous drainage filters. Water Air Soil Pollut. 1794 225. https://doi.org/10.1007/s11270-013-1794-8.

Chambers, B.J., Garwood, T.W.D., Unwin, R.J., 2000. Controlling soil water erosion and phosphorus losses from arable land in England and wales. J. Environ. Qual. 29, 145–150.

Chardon, W.J., Faassen, H.G., 1999. Soil Indicators for Critical Source Areas of Phosphorus Leaching. Programmabureau geïntegreerd bodemonderzoek, Wageningen, p. 34.

Chardon, W.J., Groenenberg, J.E., Temminghoff, E.J.M., Koopmans, G.F., 2012. Use of reactive materials to bind phosphorus. J. Environ. Qual. 41, 636–646. https://doi.org/10.2134/jeq2011.0055.

Correll, D.L., 1998. The role of phosphorus in the eutrophication of receiving waters: a review. J. Environ. Qual. 27, 261–266.

Cucarella, V., Renman, G., 2009. Phosphorus sorption capacity of filter materials used for on-site wastewater treatment determined in batch experiments-a comparative study. J. Environ. Qual. 38, 381–392. https://doi.org/10.2134/jeq2008.0192.

De Bolle, S., 2013. Phosphate Saturation and Phosphate Leaching of Acidic Sandy Soils in Flanders: Analysis and Mitigation Options. Ghent University, Ghent, p. 181.

Drizo, A., Frost, C.A., Grace, J., Smith, K.A., 1999. Physico-chemical screening of phosphate-removing substrates for use in constructed wetland systems. Water Res. 33, 3595–3602. https://doi.org/10.1016/s0043-1354(99)00082-2.

Egemose, S., Sonderup, M.J., Beinthin, M.V., Reitzel, K., Hoffmann, C.C., Flindt, M.R., 2012. Crushed concrete as a phosphate binding material: a potential new management tool. J. Environ. Qual. 41, 647–653. https://doi.org/10.2134/jeq2011.0134.

Grant, R., Laubel, A., Kronvang, B., Andersen, H.E., Svendsen, L.M., Fuglsang, A., 1996. Loss of dissolved and particulate phosphorus from arable catchments by subsurface drainage. Water Res. 30, 2633–2642. https://doi.org/10.1016/s0043-1354(96)00164-9.

Groenenberg, J.E., Chardon, W.J., Koopmans, G.F., 2013. Reducing phosphorus loading of surface water using iron-coated sand. J. Environ. Qual. 42, 250–259. https://doi.org/10.2134/jeq2012.0344.

Hsu, P.H., 1976. Comparison of iron(III) and aluminum in precipitation of phosphate from solution. Water Res. 10, 903–907.

Hylander, L.D., Kietlinska, A., Renman, G., Siman, G., 2006. Phosphorus retention in filter materials for wastewater treatment and its subsequent suitability for plant production. Bioresour. Technol. 97, 914–921. https://doi.org/10.1016/j.biortech.2005.04.026.

Klute, A., 1965. Laboratory measurement of hydraulic conductivity of saturated soil. Agronomy 9, 210–221.

Le Coustumer, S., Fletcher, T.D., Deletic, A., Barraud, S., Poelsma, P., 2012. The influence of design parameters on clogging of stormwater biofilters: a large-scale column study. Water Res. 46, 6743–6752. https://doi.org/10.1016/j.watres.2012.01.026.

Lyngsie, G., Borggaard, O.K., Hansen, H.C.B., 2014. A three-step test of phosphate sorption efficiency of potential agricultural drainage filter materials. Water Res. 51, 256–265. https://doi.org/10.1016/j.watres.2013.10.061.

McDowell, R.W., Sharpley, A.N., 2001. Approximating phosphorus release from soils to surface runoff and subsurface drainage. J. Environ. Qual. 30, 508–520.

McDowell, R.W., Sharpley, A.N., Bourke, W., 2008. Treatment of drainage water with industrial by-products to prevent phosphorus loss from tile-drained land. J. Environ. Qual. 37, 1575–1582. https://doi.org/10.2134/jeq2007.0454.

Moelants, N., Smets, I.Y., Van Impe, J.F., 2011. The potential of an iron rich substrate for phosphorus removal in decentralized wastewater treatment systems. Separ. Purif. Technol. 77, 40–45. https://doi.org/10.1016/j.seppur.2010.11.017.

Murphy, J., Riley, J.P., 1986. Citation-classic - a modified single solution method for the determination of phosphate in natural-waters. In: Current Contents/Agriculture Biology & Environmental Sciences, 16-16.

Nest, T.V., Ruysschaert, G., Vandecasteele, B., Cougnon, M., Merckx, R., Reheul, D., 2015. P availability and P leaching after reducing the mineral P fertilization and the use of digestate products as new organic fertilizers in a 4-year field trial with high P status. Agric. Ecosyst. Environ. 202, 56–67. https://doi.org/10.1016/j.agee.2014.12.012.

Penn, C., Chagas, I., Klimeski, A., Lyngsie, G., 2017. A review of phosphorus removal structures: how to assess and compare their performance. Water 583 (9). https://doi.org/10.3390/w9080583.

Penn, C.J., Bryant, R.B., Kleinman, P.J.A., Allen, A.L., 2007. Removing dissolved phosphorus from drainage ditch water with phosphorus sorbing materials. J. Soil Water Conserv. 62, 269–276.

Qin, H.L., Quan, Z., Liu, X.L., Li, M.D., Zong, Y., Wu, J.S., Wei, W.X., 2010. Phosphorus status and risk of phosphate leaching loss from vegetable soils of different planting years in suburbs of changsha, China. Agric. Sci. China 9, 1641–1649. https://doi.org/10.1016/s1671-2927(09)60261-3.

R_Core_Team, 2017. R: a Language and Environment for Statistical Computing.

Salomez, J., De Bolle, S., Hofman, G., De Neve, S., 2006. In: D.o.S.M (Ed.), Afbakening van de fosfaatverzadigde gebieden in Vlaanderen op basis van een kritische fosfaatverzadigingsgraad van 35%. Ghent University.

Sanford, W.E., Steenhuis, T.S., Parlange, J.Y., Surface, J.M., Peverly, J.H., 1995. Hydraulic conductivity of gravel and sand as substrates in rock-reed filters. Ecol. Eng. 4, 321–336. https://doi.org/10.1016/0925-8574(95)00004-3.

Schoumans, O.F., Chardon, W.J., 2015. Phosphate saturation degree and accumulation of phosphate in various soil types in The Netherlands. Geoderma 237, 325–335. https://doi.org/10.1016/j.geoderma.2014.08.015.

Sims, J.T., Simard, R.R., Joern, B.C., 1998. Phosphorus loss in agricultural drainage: historical perspective and current research. J. Environ. Qual. 27, 277–293.

Svanback, A., Ulen, B., Etana, A., 2014. Mitigation of phosphorus leaching losses via subsurface drains from a cracking marine clay soil. Agric. Ecosyst. Environ. 184, 124–134. https://doi.org/10.1016/j.agee.2013.11.017.

Ulen, B., Bechmann, M., Folster, J., Jarvie, H.P., Tunney, H., 2007. Agriculture as a phosphorus source for eutrophication in the north-west European countries, Norway, Sweden, United Kingdom and Ireland: a review. Soil Use Manag. 23, 5–15. https://doi.org/10.1111/j.1475-2743.2007.00115.x.

van der Salm, C., Chardon, W.J., Koopmans, G.F., van Middelkoop, J.C., Ehlert, P.A.I., 2009. Phytoextraction of phosphorus-enriched grassland soils. J. Environ. Qual. 38, 751–761. https://doi.org/10.2134/jeq2008.0068.

Van Hecke, E., 2003. Ruimtegebruik in Vlaanderen. Studie uitgevoerd in opdracht van de Vlaamse Milieumaatschappij. Instituut voor sociale en economische geografie, p. 54.

Wendling, L.A., Blomberg, P., Sarlin, T., Priha, O., Arnold, M., 2013. Phosphorus sorption and recovery using mineral-based materials: sorption mechanisms and potential phytoavailability. Appl. Geochem. 37, 157–169. https://doi.org/10.1016/j.apgeochem.2013.07.016.

Weng, L.P., Van Riemsdijk, W.H., Hiemstra, T., 2012. Factors controlling phosphate interaction with iron oxides. J. Environ. Qual. 41, 628–635. https://doi.org/10.2134/jeq2011.0250.

Westholm, L.J., 2006. Substrates for phosphorus removal - potential benefits for on-site wastewater treatment? Water Res. 40, 23–36. https://doi.org/10.1016/j.watres.2005.11.006.